PHOTONIC SENSORS / Vol. 15, No. 3, 2025: 250318

Simultaneous Measurement of Liquid Level and Refractive Index Employing a Side-Polished Spiral Polymer Optical Fiber Based SPR Sensor

Chuanxin TENG[1*], Rongping YANG[1], Rui MIN[2], Jiangrong LU[3], Shijie DENG[1], Minmin XUE[1], Ming CHEN[1], Libo YUAN[1], and Xuehao HU[4]

[1]*Guangxi Key Laboratory of Optoelectronic Information Processing, Guilin University of Electronic Technology, Guilin 541004, China*

[2]*Center for Cognition and Neuroergonomics, State Key Laboratory of Cognitive Neuroscience and Learning, Beijing Normal University, Zhuhai 519087, China*

[3]*School of Materials Science and Engineering, Guilin University of Electronic Technology, Guilin 541004, China*

[4]*Department of Electromagnetism and Telecommunication, University of Mons, Mons 7000, Belgium*

[*]Corresponding author: Chuanxin TENG E-mail: cxteng@guet.edu.cn

Abstract: The work describes a surface plasmon resonance (SPR) sensor that measures the liquid level and refractive index (RI) simultaneously. The sensor is fabricated by a polymer optical fiber (POF) with a side-polished spiral structure. The POF is wound around a plastic rod with the same pitch and polished into a series of separated side-polished areas to form the sensor probe. Afterwards, the polished surfaces are coated with a gold layer to construct the SPR sensor. The proposed sensor can provide multi-point liquid-level measurement besides RI sensing. The influences of structural parameters such as the bending radius, polishing depth, and pitch on the sensing performance are experimentally studied. The experimental results indicate that the RI could be determined by employing the SPR wavelength shift, and the RI sensitivity of 1862 nm/RIU within the 1.34–1.40 range is obtained. Moreover, the SPR peak's depth variation can be utilized to monitor the liquid level, and the sensor can provide adjustable resolution and a measurement range for liquid level sensing. With its simple fabrication, low cost, and flexible sensing ability, this sensor probe is suitable for the usage in biochemical applications.

Keywords: Surface plasmon resonance sensor; side-polished spiral structure; polymer optical fiber; refractive index sensing; liquid level sensing.

Citation: Chuanxin TENG, Rongping YANG, Rui MIN, Jiangrong LU, Shijie DENG, Minmin XUE, *et al*. "Simultaneous Measurement of Liquid Level and Refractive Index Employing a Side-Polished Spiral Polymer Optical Fiber Based SPR Sensor," *Photonic Sensors*, 2025, 15(3), 250318.

1. Introduction

Liquid level monitoring is critical and extensively demanded in automated production processes in industries, such as food, beverage, the chemical, and pharmaceutical. In contrast to the traditional electrical measuring approaches, an optical fiber sensor (OFS) is characterized by its small size, corrosion resistance, anti-electromagnetic interference, and high insulation strength, enabling it

Received: 9 November 2023 / Revised: 1 January 2024

DOI: 10.1007/s13320-025-0723-y
Article type: Regular

to be applied for liquid level monitoring in hazardous environments. Considering the operating principle, optical fiber-based liquid level sensors such as the interference type [1, 2], grating type [3, 4], and surface plasmon resonance (SPR) type [5–7] have been reported. The multi-parameter OFS has become more and more in demand in recent years, as the measured surroundings have grown more and more complicated. For instance, in biopharmaceutical and environmental monitoring, both the quantity and refractive index (RI) of the measured sample are needed to be detected. In the above optical fiber-based liquid level sensing types, the SPR type is capable of monitoring subtle changes in the external RI [8], which is more suitable for designing as a bi-parametric sensor to monitor both the liquid level and RI.

The SPR phenomenon can be described as follows: the incident light excites coherent oscillations of the metal's free electrons at the metal-dielectric interface and produces the surface plasma waves; the SPR happens when the incident light and the surface plasma wave vectors meet the matching conditions. SPR sensors are characterized by their real-time detection, label-free, and high sensitivity. To date, there are various types of optical fiber-based SPR sensors, such as D-shaped structures [9, 10], U-shape structures [11], tapered structures [12, 13], and hetero-core structures [14]. There have also been several reports of optical fiber-based SPR sensors that can measure multiple parameters simultaneously in the past few years. The measured multiple parameters include the nitrate concentration and temperature [15]; seawater salinity, temperature, and pressure [16]; temperature and magnetic field intensity [17]; RI and temperature [18–25]; liquid level and RI [5]. Most of the sensors mentioned above, however, are brittle and susceptible to damage because they are made by the glass optical fibers.

The polymer optical fiber (POF) is widely recognized for its benefits of the light weight, flexibility, large core size, easy operation, and low cost [26], which is a candidate for the glass optical fiber and has been used for liquid level sensing. In recent years, Teng *et al*. [6] proposed and realized an SPR sensor to measure both of the liquid level and RI by using the POF with the micro-hole structure. However, the fabrication of micro-holes makes the POF brittle and easy to be fractured. Besides, it is difficult for the liquid to enter and come out of the micro-holes entirely, which will influence the measurement accuracy. Subsequently, the same group presented an SPR sensor from the side-polished POF to determine the changes in the continuous liquid level and liquid RI [7]. However, due to the limitation of the sensor structure, the measurement range for liquid level sensing is limited.

In order to improve the measurement range of the liquid level and realize the simultaneous measurement of the liquid level and RI, this work presented an equal-pitch spiral side-polished POF based SPR sensor. The sensing regions of the proposed probe were dispersed on the separated polished surfaces of the spiral POF. Based on this structure, the proposed sensor could provide multi-point liquid-level measurement with the tunable resolution and range. For analyzing the response characteristics of the presented sensor, a three-layer model was performed for the liquid level and RI responses. The effects of the bending radius, polishing depth, and fiber pitch on sensing characteristics were investigated experimentally. The experimental results indicated that the SPR wavelength shift was used to determine the RI, and the SPR peak's depth variation could be utilized to detect the liquid level. Therefore, it was possible to detect the liquid level and RI simultaneously by monitoring the SPR peak's wavelength shift and depth change. In the RI range of 1.34–1.40, the presented sensor exhibited the sensitivity of

1 862 nm/RIU for RI sensing. The advantages of the suggested sensor include its simple fabrication, inexpensive cost, and flexible sensing ability, which may be used in the biochemical industries.

2. Structure and working principle

Figure 1 presents the schematic and cross-sectional view of the probe structure. It consists of an equal-pitch spiral side-polished POF covered with a layer of the gold film. In Fig. 1, R represents the bending radius, L represents the polishing length, d represents the diameter of the POF, D represents the remaining fiber diameter, h is the polishing depth, and $x = D - d/2$ represents the distance between the fiber axis and the center of the polishing area. A POF (CK-20, ESKA, Japan) with a 500 μm diameter was employed for fabricating the probe.

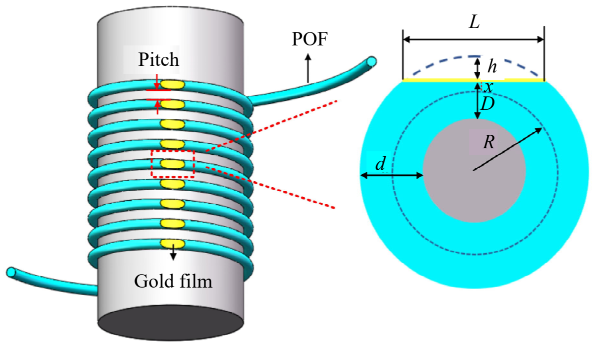

Fig. 1 Schematic diagram and cross-sectional view of the structure of the presented sensor.

The normalized transmission spectra for the liquid level and RI sensing can be analyzed with a three-layer model (the fiber core, gold film, and measured liquid), which can be expressed as [27]

$$T = \frac{\int_{\theta_{cr}}^{\pi/2} R_G^{N_{ref}(\theta)} P(\theta) \mathrm{d}\theta}{\int_{\theta_{cr}}^{\pi/2} P(\theta) \mathrm{d}\theta} \tag{1}$$

where $\theta_{cr} = \sin^{-1}(n_2/n_1)$ is the incident light critical angle, n_2 is the RI of the fiber cladding, and n_1 is the RI of the fiber core. R_G is the reflectivity [24] at the interface between the fiber core and gold film, and $P(\theta)$ is the modal power for light incidence angle θ [24]. $N_{ref}(\theta) = L/2D\tan\theta$ is the number of light reflection on each polished surface [27], and $L = 2\sqrt{-h + 2Rh + dh}$ is the polishing length.

The fiber core RI distribution changes with the bending of the POF, and its effective RI can be expressed as [28]

$$n_{eq} = n_1 \left\{1 - \frac{n_1^2 x}{2R}\left[\rho_{12} - v(\rho_{11} + \rho_{12})\right]\right\}\left(1 + \frac{x}{R}\right) \tag{2}$$

where the POF has an elasticity coefficient ρ_{11} of 0.30, ρ_{12} of 0.20, and Poisson's ratio v of 0.34 [29].

Figure 2 presents the RI sensing simulation results of the probe. In the simulation, gold film's permittivity was determined by using Drude's model [30], and its thickness was set to 50 nm. The θ was 70°, R was 7.75 mm, h was 100 μm, d was 500 μm, D was 400 μm, x was 150 μm, n_1 was 1.49, and n_2 was 1.41. M was the polished surface number immersed in the liquid. As demonstrated in Fig. 2, the SPR peak's wavelength red-shifts and the intensity increases with the RI. Therefore, the wavelength can be employed to determine the RI of solutions. The relationships between the resonance wavelength and RI for the probe with different liquid levels are given in Fig. 2(d), and it can be seen that the liquid level has little influence on the RI sensing.

When the liquid level changes, more polished POF coated with the gold film will be immersed, changing the length of the fiber that excites the SPR effect, which in turn alters the quantity of reflection and the SPR peak's depth. Figure 3 presents the liquid level sensing simulation results of the presented sensor with nine polished surfaces. It presents that the wavelength positions are 516 nm and 559 nm at RIs of 1.34 and 1.36, respectively. Additionally, it is shown that with the increasing liquid levels, the SPR peak's depth increases accordingly. Therefore, it is concluded from the simulation results that the presented sensor can monitor the liquid level and RI simultaneously.

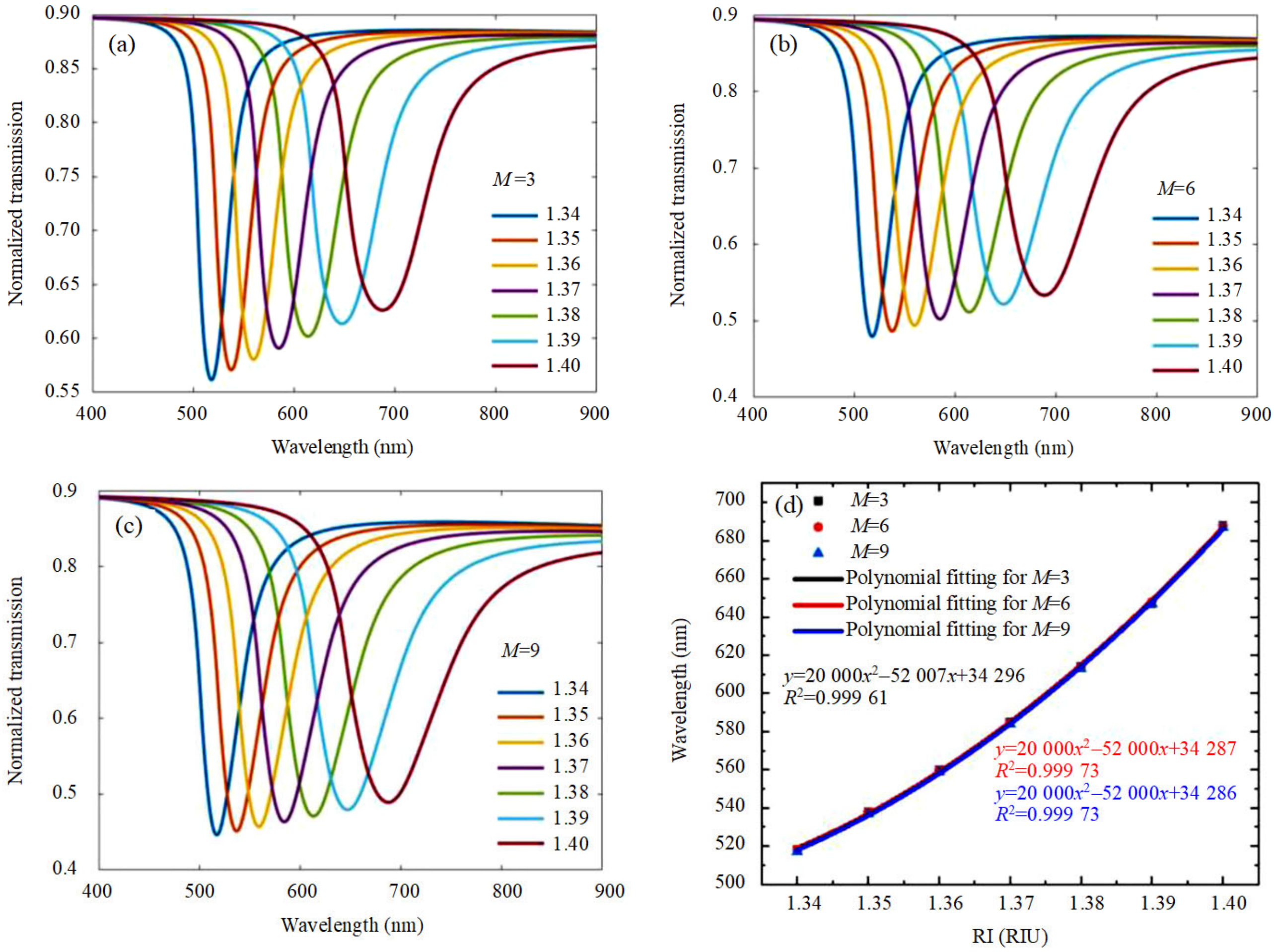

Fig. 2 Simulation results of RI sensing and the relationships between the wavelength and RI in the RI range of 1.34–1.40 for the probe at different liquid levels.

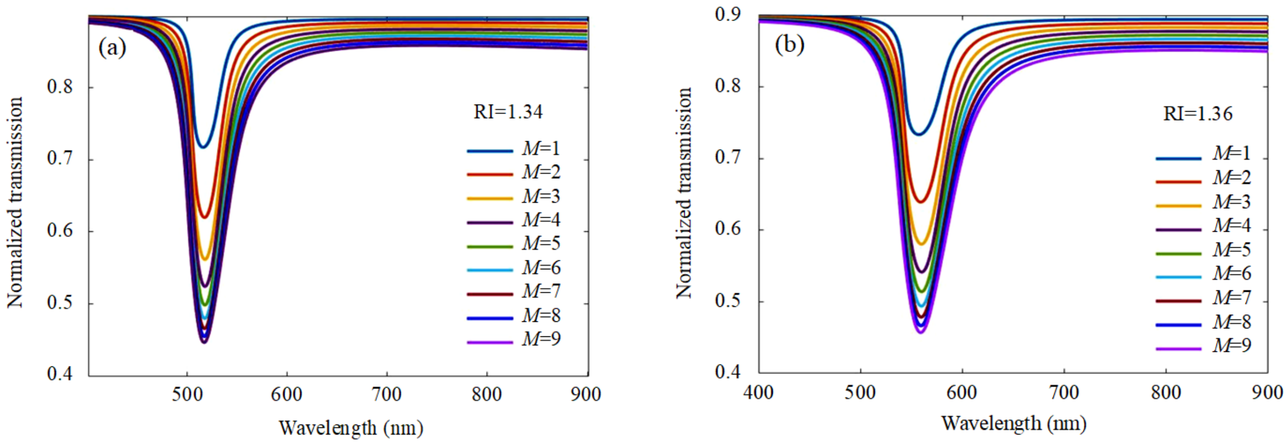

Fig. 3 Simulation results for liquid level sensing with nine polished surfaces for the sensor at RIs of 1.34 and 1.36.

3. Sensor probe preparation

The preparation process for the sensor is presented in Fig. 4. Firstly, the POF was wound around a plastic rod with the equal pitch and fixed to the rod with the glue to obtain a stable spiral POF structure. Secondly, a three-dimensional (3D) printer was used to print a groove mold, in which the round rod can be placed. A rectangular rod with the sandpaper was utilized to polish the POF to obtain a side-polished structure on the spiral POF. It is worth noting that the polishing rod should be longer than the width of the mold, and the POF should be polished along its axis, which is shown in Fig. 4(b). The polishing depth of the probe could be controlled by setting the groove depth of the mold. During the polishing process, the light source and spectrometer were connected to the POF, and the spectrum was monitored in real time in order to improve the repeatability and reproducibility of the probe. The accuracy of the polishing depth was about ±10 μm. In our experiment, nine polished surfaces along the circle rod were fabricated on the spiral POF probe. Thirdly, to obtain a smooth polished surface, the polished surface was further polished by using the alumina polishing paste for about 3 min–4 min. After that, the alumina polishing paste was washed off with an ultrasonic cleaner, and the probe should be dried. Finally, the polished surfaces were covered with a gold film by using a magnetron sputtering apparatus. The sputtering current and duration time were 25 mA and 70 s, respectively, and a gold film with a thickness of 50 nm was fabricated on the polished region. The coating thickness could be monitored by a film thickness monitor.

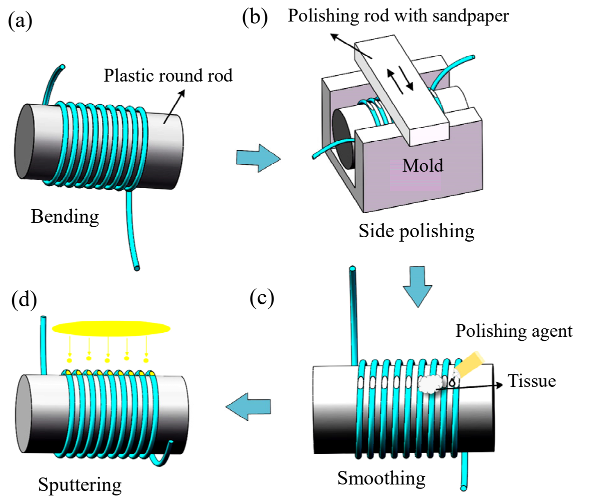

Fig. 4 Schematic diagram of the probe preparation process: (a) bending, (b) side polishing, (c) smoothing, and (d) sputtering.

4. Experimental results and discussion

Figure 5 presents the liquid level and RI sensing experimental setup. A 360 nm–2500 nm wavelength-range halogen light source (HL2000, ideaoptics, China) was connected to the probe. The other end of POF was connected to a spectral analyzer (NOVA, ideaoptics, China) to record the transmission spectra. The measured samples were made of a mixture of different proportions of glycerol and water solutions with RI values of 1.34–1.40. Their RIs were determined with an Abbe refractometer. The probe was fixed inside a container vertically, and a ruler was used to calibrate the liquid level.

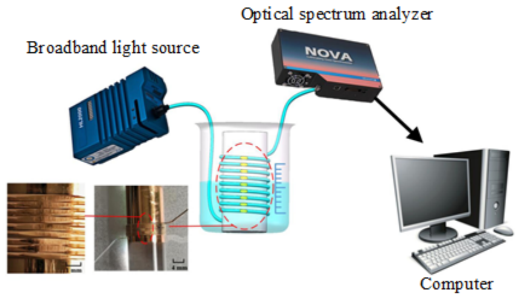

Fig. 5 Schematic diagram of experimental setup.

For the measurement of RI, the polished surfaces were immersed in the measured samples, and the transmitted spectra of different RIs were recorded. It is worth noting that before changing samples for measurement, it is necessary to clean and dry the probe. For the measurement of the liquid level, it was needed to record the transmitted spectra of each liquid level when each of the polished surface was immersed in the measured sample. The liquid level below the first polished surface was assumed to be zero. The air transmitted spectrum was used to normalize the transmitted spectra of the liquid level and RI, and the obtained transmitted spectra should be smoothed.

Figure 6 presents the RI sensing experimental results with different bending radii. The probes with different bending radii were fabricated with a pitch of 0.5 mm and a polishing depth of 50 μm. In the experiment, only three polished surfaces (M=3) were immersed in the measured liquid. Figures 6(a)–6(c) display that all probes' SPR wavelength positions shift to the long wavelengths when the RI increases. Also, the probe with an R of 7.75 mm had a better spectrum visibility, which made it easy to distinguish the SPR peak position. The relationships between the wavelength shift and RI for various probes are presented in Fig. 6(d). It can be seen although the sensitivity of the probe with a 7.75 mm bend radius is slightly lower, the linearity of the probe is the best. Therefore, the probe with a 7.75 mm bending radius was chosen for the subsequent study by considering its better spectrum visibility and linearity.

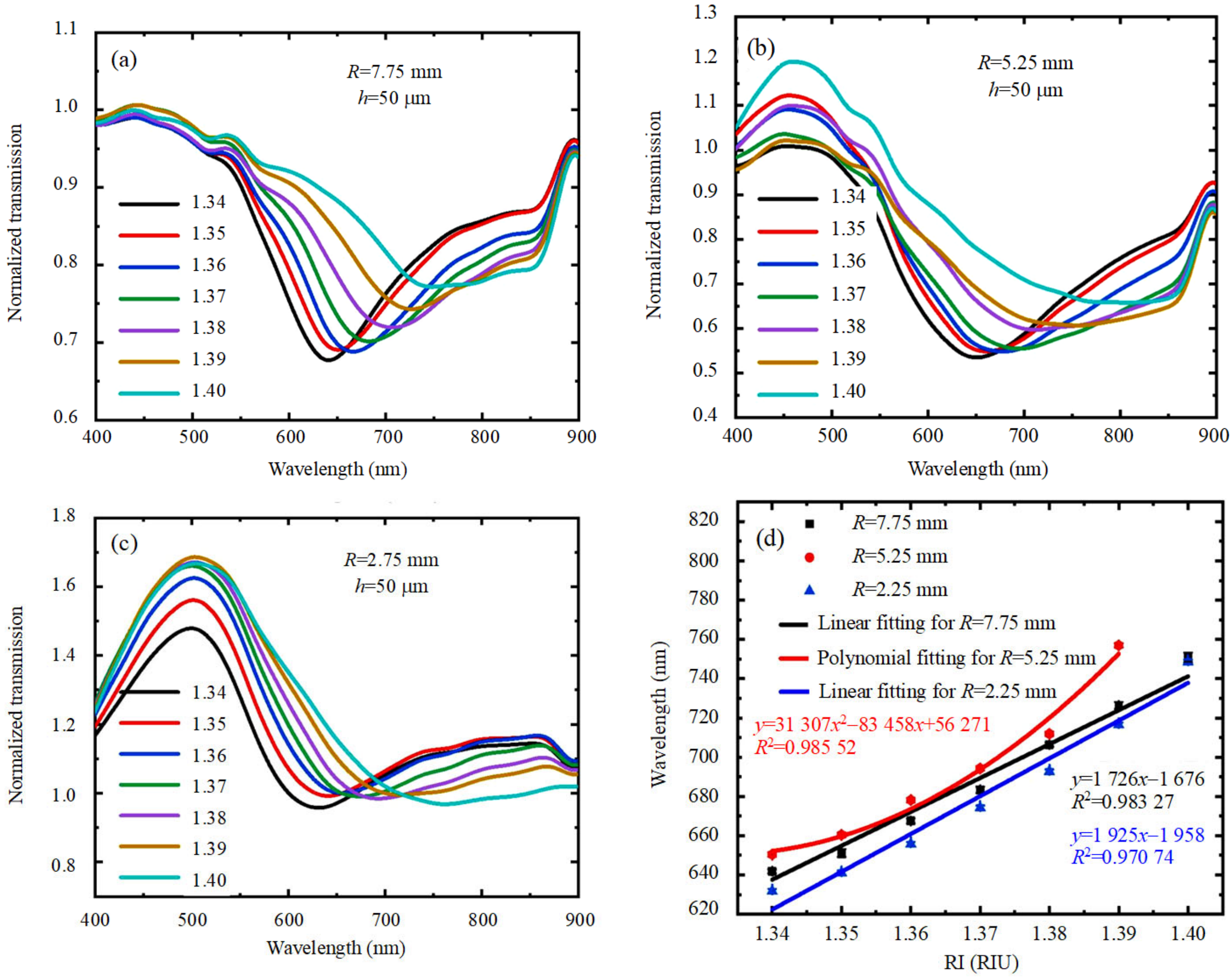

Fig. 6 Results of RI sensing experiments with various bending radii of (a) 7.75 mm, (b) 5.25 mm, and (c) 2.75 mm; (d) the relationships between the wavelength shift and RI for different probes.

Figure 7 exhibits the RI sensing experimental results with different polishing depths. Probes with various polishing depths of 100 μm and 150 μm were prepared with the same pitch of 0.5 mm and radius of 7.75 mm. Three polished surfaces were immersed in the liquid. Figures 7(a) and 7(b) show that the position in the normalized transmitted spectra is red-shifted as the RI increases. Figure 7(c) presents the SPR peak's full width at half maximum (FWHM) for probes with different polished depths in the RI of 1.34. It can be seen that the probe with polishing the depth of 100 μm has the minimum FWHM. The SPR peak of the proposed probe broadened with increasing RI in the range of 1.34–1.40. For the RI of 1.40, the minimum values of the SPR peaks for the two probes with R of 5.25 mm, h of 50 μm and R of 7.75 mm, h of 150 μm have been already indistinguishable. Thus, for these two probes, the RI ranges were reduced to 1.34–1.39. Figure 7(d) shows the relationship between the wavelength shift and the RI, the results indicate that the probes with polishing depths of

50 μm and 100 μm have good linearity, and the sensitivity for the probe with the 100 μm polishing depth is 1862 nm/RIU, which is higher than that with 50 μm. Therefore, the probe with a 7.75 mm bending radius and a 100 μm polishing depth was chosen for the subsequent study.

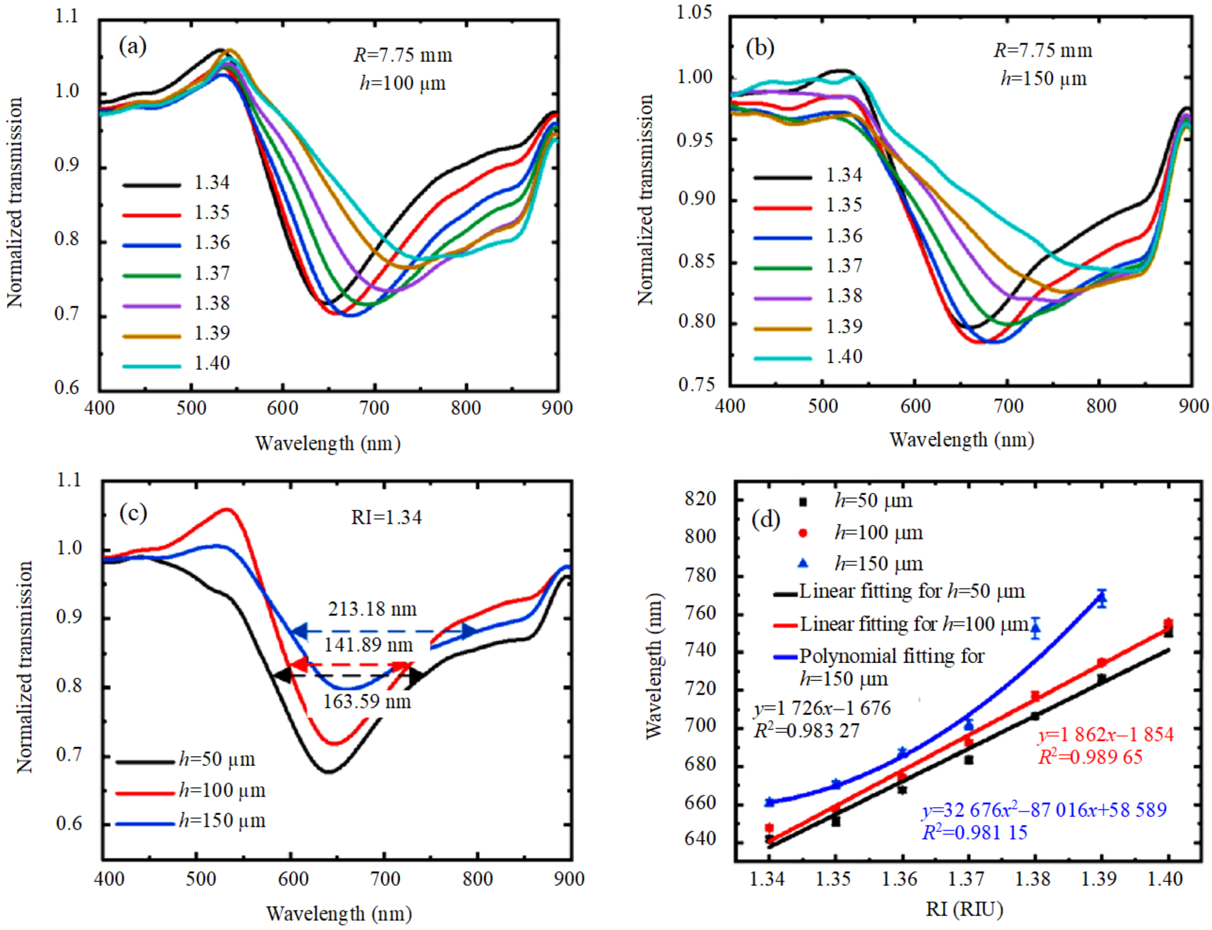

Fig. 7 Experimental results of RI sensing with various polishing depths of (a) 100 μm and (b) 150 μm; (c) results of RI sensing experiments for probes with varied polishing depths when RI is 1.34; (d) relationships between the wavelength shift and RI for different probes.

To check the capability of the presented probe to measure the liquid level. Probes were fabricated with pitches of 0.5 mm, 2 mm, and 4 mm, a bending radius of 7.75 mm, and a polishing depth of 100 μm. Figure 8 shows these probes' liquid-level sensing characteristics at an RI of 1.34. It is evident that immersing the polished surfaces in the measured solution could cause a significant reduction in the intensity of the SPR peak. The decrease in the SPR peak might be caused by the combined effects of the increased polished length and the corresponding macrobend loss. It can be seen that the resonance wavelengths of the SPR peaks were all around 655 nm, which indicated that the changes in the pitch and liquid level had little effect on the RI test. Figures 8(b), 8(d), and 8(f) show the relationships between the SPR peak's intensity and liquid level for varied probes. The results also show that the probes could provide the multi-point liquid level measurement with the flexible resolution and measurement range. It can also be seen that the change in the SPR spectrum intensity was irregular with the increasing of M, these irregular variations might mainly result from the inconsistency of the polished depth for each polished region and the gold film thickness on the polished area, which needs to be further studied.

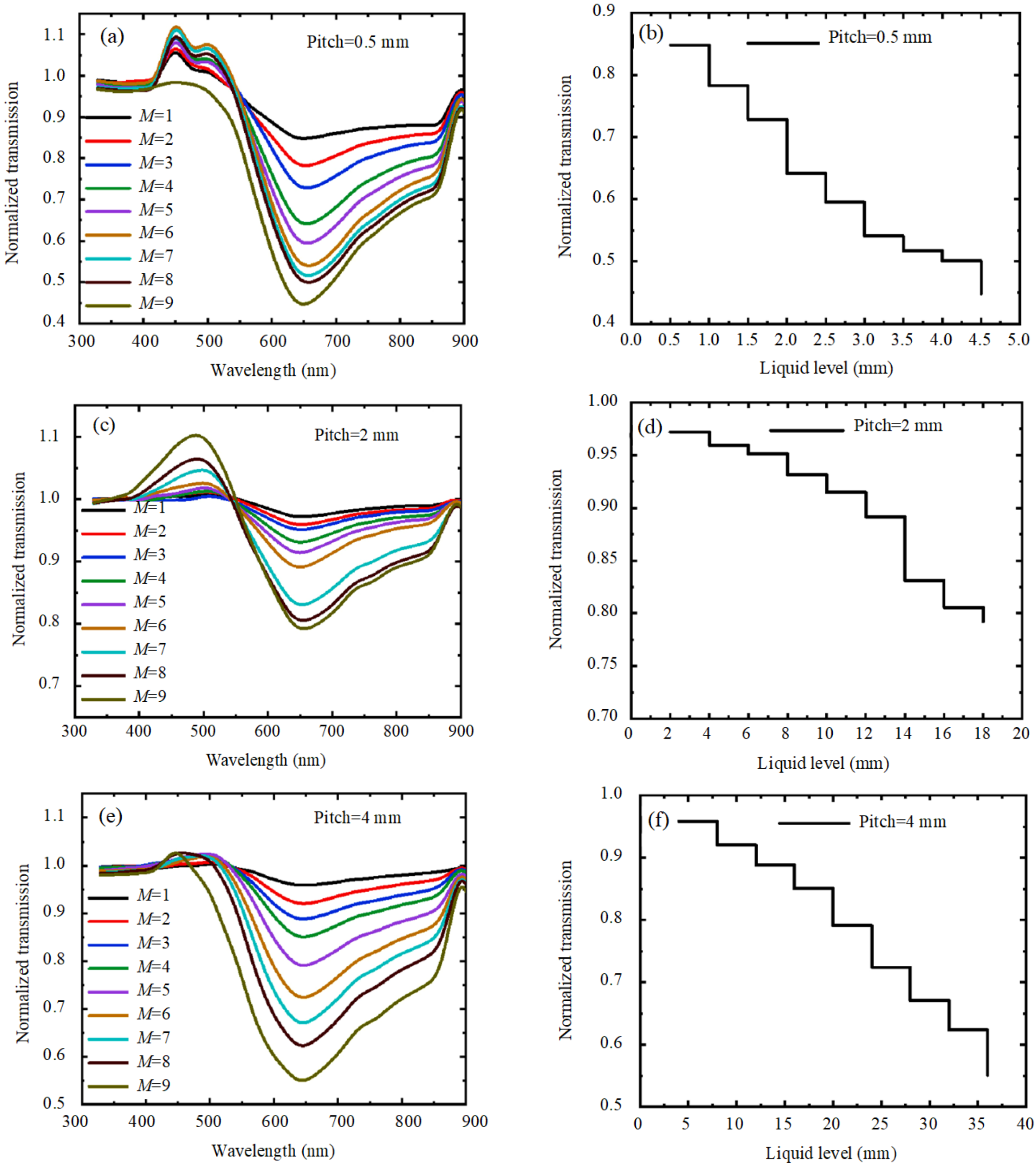

Fig. 8 Experimental results of liquid level sensing with varied pitches of (a) 0.5 mm, (c) 2 mm, and (e) 4 mm, when the liquid RI is 1.34; (b), (d), and (f) are the relationships between the SPR peak's intensity and liquid level for different probes.

Figure 9(a) presents the liquid level sensing for the probe with a 2 mm pitch at an RI of 1.36. Compared with Fig. 8(c), the resonance wavelength red-shifts to around 696 nm, and the wavelength position can be used for determining the RI. Additionally, Fig. 9(b) shows that as more polished surfaces are immersed in the solution, the SPR peak intensity decreases. Thus, it is possible to determine the liquid level by observing the intensity variation of the SPR peak at 696 nm.

To analyze the liquid level effect on the RI sensing characteristics, RI measurement was performed on the probe with a 2 mm pitch at the liquid levels of 12 mm and 18 mm, respectively. Figure 10 shows the experimental results. It is evident that the SPR wavelength red-shifted with the increasing RI, and the SPR peak was deeper at the liquid level of 18 mm. Figure 10(d) shows the RI responses of the probe at liquid levels of 12 mm and 18 mm. It indicates that the variations in the liquid level almost had no impact on RI sensing performance, which is consistent with the simulation results. Thus, the presented sensor can measure liquid level and RI simultaneously with low cross-sensitivity.

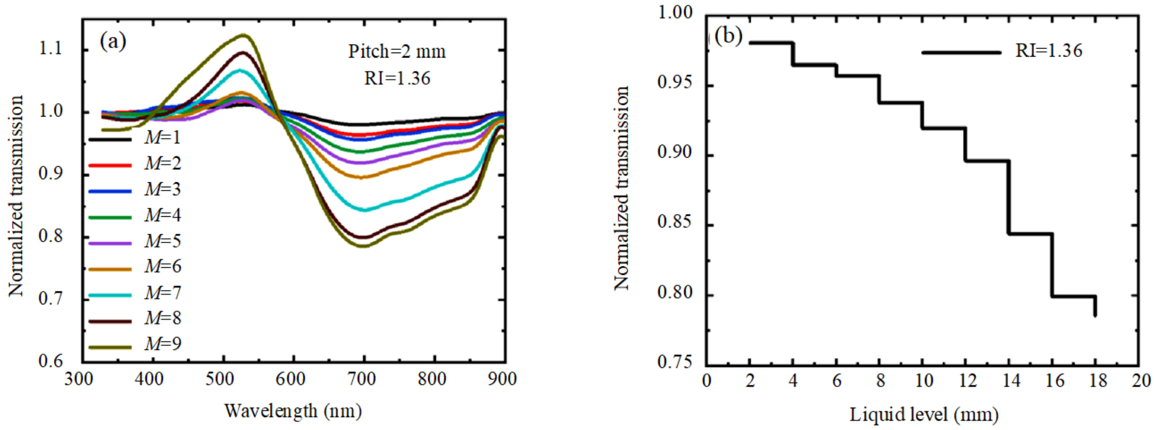

Fig. 9 Experimental results of (a) the liquid level sensing with a probe pitch of 2 mm at an RI of 1.36; (b) the relationship between the liquid level and the SPR peak's intensity.

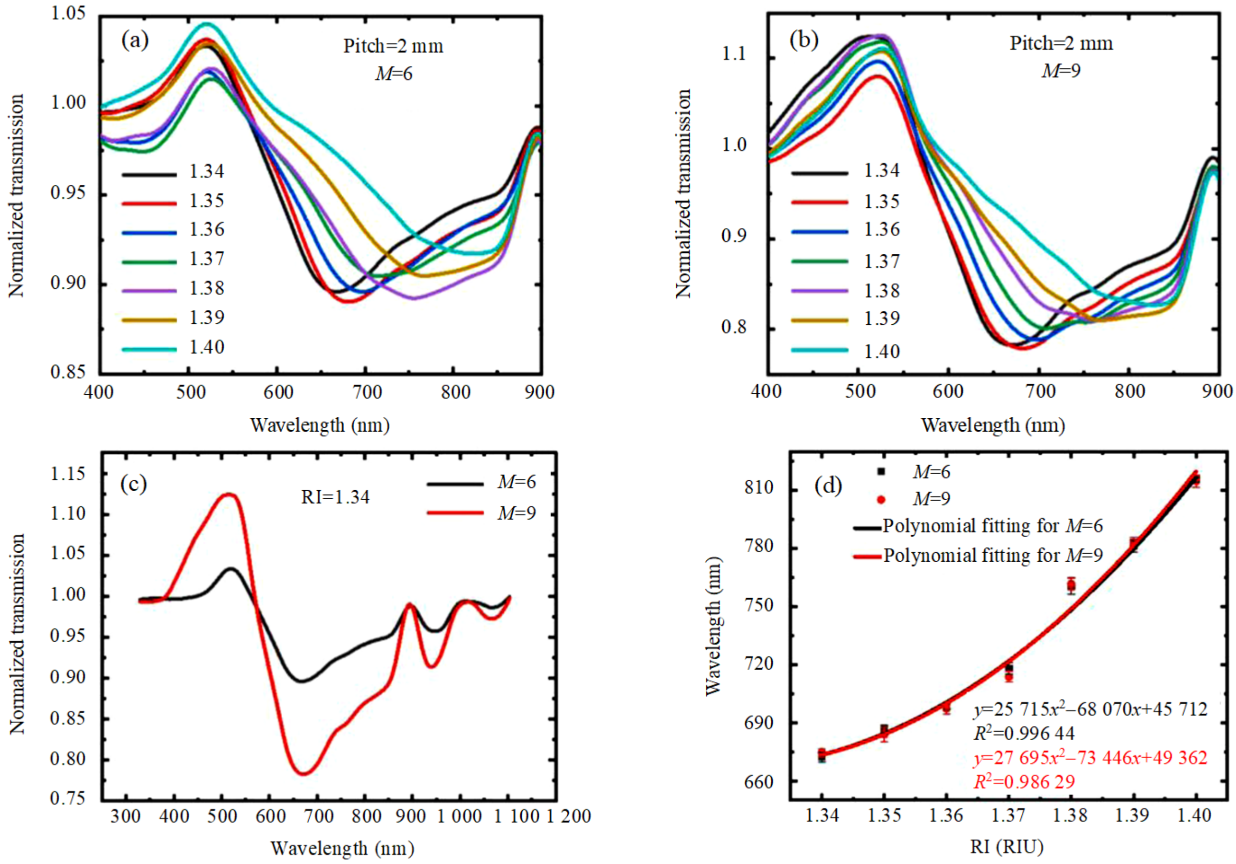

Fig. 10 Experimental results of RI sensing at (a) 12 mm (M=6) and (b) 18 mm (M=9) liquid levels for the probe with a 2 mm pitch; (c) the RI sensing experimental results of the probe at different liquid levels when RI is 1.34; (d) the relationships between the wavelength and RI in the RI range of 1.34–1.40 for the probe at different liquid levels.

5. Conclusions

A side-polished spiral POF based SPR sensor that measures the liquid level and RI was presented and fabricated. A theoretical model was established to investigate the liquid level and RI responses of the presented sensor. The simulation results showed that the SPR wavelength red-shifted with the RI and the SPR peak depth changed with the liquid level. The effects of the bending radius and polishing depth on the RI sensing characteristics and the influence of optical fiber pitch on the liquid level sensing characteristics were studied. Experimental results showed the sensor with a 100 μm polishing depth and a 7.75 mm bending radius exhibited better performance. The sensor demonstrated the sensitivity of 1862 nm/RIU in the RI range of 1.34–1.40. Besides RI measurement, the presented sensor can also perform liquid level sensing. The results showed that the measurement resolution and range could be flexibly adjusted by altering the spiral fiber pitch. The presented sensor probe has the advantages of the simple fabrication, low cost, and flexible sensing ability, making it suitable for biochemical applications.

Acknowledgment

This work was supported by the Guangxi Natural Science Foundation, China (Grant Nos. 2023GXNSFDA026040 and ZY23055018); National Natural Science Foundation of China (Grant Nos. 62365003, 62364006, and U23A20282); the Fonds de la Recherche Scientifique under the Postdoctoral Researcher Grant (Chargé de Recherches), Belgium to Xuehao HU; the Innovation Project of Guilin University of Electronic Technology Graduate Education, China (Grant No. 2024YCXS202).

Declarations

Conflict of Interest Libo YUAN is an editorial board membe for Photonic Sensors and was not involved in the editorial review, or the decision to publish this article. All authors declare that there are no competing interests.

References

[1] F. Zhang, S. Li, X. Yan, X. Zhang, F. Wang, T. Suzuki, *et al.*, "A refractive index sensitive liquid level monitoring sensor based on multimode interference," *Photonics*, 2020, 7(4): 89.

[2] M. Galarza, R. A. Perez-Herrera, D. Leandro, A. Judez, and M. López-Amo, "Spatial-frequency multiplexing of high-sensitivity liquid level sensors based on multimode interference micro-fibers," *Sensors and Actuators A: Physical*, 2020, 307: 111985.

[3] A. L. Ricchiuti, D. Barrera, A. Urrutia, J. Goicoechea, F. J. Arregui, and S. Sales, "Continuous liquid-level sensor based on a long-period grating and microwave photonics filtering techniques," *IEEE Sensors Journal*, 2016, 16(6): 1652–1658.

[4] C. A. R. Díaz, A. G. Leal-Junior, P. S. B. André, P. F. da C. Antunes, M.J. Pontes, A. Frizera-Neto, *et al.*, "Liquid level measurement based on FBG-embedded diaphragms with temperature compensation," *IEEE Sensors Journal*, 2018, 18(1): 193–200.

[5] M. del C. Alonso-Murias, J. S. Velazquez-Gonzalez, and D. Monzon-Hernandez, "SPR fiber tip sensor for the simultaneous measurement of refractive index, temperature, and level of a liquid," *Journal of Lightwave Technology*, 2019, 37(18): 4808–4814.

[6] C. Teng, Y. Wang, R. Min, S. Deng, H. Deng, Y. Li, *et al.*, "Plastic optical fiber based SPR sensor for simultaneous measurement of refractive index and liquid level," *IEEE Sensors Journal*, 2022, 22(7): 6677–6684.

[7] C. Teng, S. Ying, R. Min, S. Deng, H. Deng, M. Chen, *et al.*, "Side-polish plastic optical fiber based SPR sensor for refractive index and liquid-level sensing," *Sensors*, 2022, 22(16): 6241.

[8] J. Homola, "Surface plasmon resonance sensors for detection of chemical and biological species," *Chemical Reviews*, 2008, 108(2): 462–493.

[9] S. F. Wang, M. H. Chiu, and R. S. Chang,

"Numerical simulation of a D-type optical fiber sensor based on the Kretchmann's configuration and heterodyne interferometry," *Sensors and Actuators B: Chemical*, 2006, 114(1): 120–126.

[10] N. Cennamo, L. Pasquardini, F. Arcadio, L. E. Vanzetti, A. M. Bossi, and L. Zeni, "D-shaped plastic optical fibre aptasensor for fast thrombin detection in nanomolar range," *Scientific Reports*, 2019, 9(1): 18740.

[11] D. Paul, S. Dutta, and R. Biswas, "LSPR enhanced gasoline sensing with a U-bent optical fiber," *Journal of Physics D: Applied Physics*, 2016, 49(30): 305104.

[12] R. K. Verma, A. K. Sharma, and B. D. Gupta, "Modeling of tapered fiber-optic surface plasmon resonance sensor with enhanced sensitivity," *IEEE Photonics Technology Letters*, 2007, 19(22): 1786–1788.

[13] R. K. Verma, A. K. Sharma, and B. D. Gupta, "Surface plasmon resonance based tapered fiber optic sensor with different taper profiles," *Optics Communications*, 2008, 281(6): 1486–1491.

[14] W. Zhu, Q. Huang, Y. Wang, E. Lewis, and M. Yang, "Enhanced sensitivity of heterocore structure surface plasmon resonance sensors based on local microstructures," *Optical Engineering*, 2018, 57(7): 076105.

[15] Y. N. Zhang, E. Siyu, B. R. Tao, Q. L. Wu, and B. Han, "Reflective SPR sensor for simultaneous measurement of nitrate concentration and temperature," *IEEE Transactions on Instrumentation and Measurement*, 2019, 68(11): 4566–4574.

[16] Y. Zhao, Q. Wu, and Y. Zhang, "Simultaneous measurement of salinity, temperature and pressure in seawater using optical fiber SPR sensor," *Measurement*, 2019, 148: 106792.

[17] B. Li, F. Zhang, X. Yan, X. Zhang, F. Wang, and T. Cheng, "An optical fiber-based surface plasmon resonance sensor for simultaneous measurement of temperature and magnetic field intensity," *IEEE Transactions on Instrumentation and Measurement*, 2022, 71: 1–7.

[18] S. Weng, L. Pei, C. Liu, J. Wang, J. Li, and T. Ning, "Double-side polished fiber SPR sensor for simultaneous temperature and refractive index measurement," *IEEE Photonics Technology Letters*, 2016, 28(18): 1916–1919.

[19] J. S. Velázquez-González, D. Monzón-Hernández, D. Moreno-Hernández, F. Martínez-Piñón, and I. Hernández-Romano, "Simultaneous measurement of refractive index and temperature using a SPR-based fiber optic sensor," *Sensors and Actuators B: Chemical*, 2017, 242: 912–920.

[20] L. Liu, Z. Liu, Y. Zhang, and S. Liu, "V-shaped micro-structure optical fiber surface plasmon resonance sensor for the simultaneous measurement of the refractive index and temperature," *Optics Letters*, 2019, 44(20): 5093.

[21] L. Liu, J. Zheng, S. Deng, L. Yuan, and C. Teng, "Parallel polished plastic optical fiber-based SPR sensor for simultaneous measurement of RI and temperature," *IEEE Transactions on Instrumentation and Measurement*, 2021, 70: 1–8.

[22] Y. Zhang, H. Chen, M. Wang, Y. Liu, X. Fan, Q. Chen, *et al*., "Simultaneous measurement of refractive index and temperature of seawater based on surface plasmon resonance in a dual D-type photonic crystal fiber," *Materials Research Express*, 2021, 8(8): 085201.

[23] Q. Zhang, H. Liu, B. Li, F. Zhang, X. Yan, X. Zhang, *et al*., "A dual-channel surface plasmon resonance sensor for the liquid refractive index and temperature measurement based on hollow-core fiber," *IEEE Sensors Journal*, 2022, 22(8): 7785–7791.

[24] C. Teng, P. Shao, S. Li, S. Li, H. Liu, H. Deng, *et al*., "Double-side polished U-shape plastic optical fiber based SPR sensor for the simultaneous measurement of refractive index and temperature," *Optics Communications*, 2022, 525: 128844.

[25] Z. Yin, X. Jing, G. Bai, B. Wu, Z. Gao, C. Liu, *et al*., "Experimental study of dual-parameter SPR sensor with integrated sensing channel," *IEEE Sensors Journal*, 2023: 1.

[26] R. He, C. Teng, S. Kumar, C. Marques, and R. Min, "Polymer optical fiber liquid level sensor: a review," *IEEE Sensors Journal*, 2022, 22(2): 1081–1091.

[27] J. S. Velázquez-González, D. Monzón-Hernández, F. Martínez-Piñón, D. A. May-Arrioja, and I. Hernández-Romano, "Surface plasmon resonance-based optical fiber embedded in PDMS for temperature sensing," *IEEE Journal of Selected Topics in Quantum Electronics*, 2017, 23(2): 126–131.

[28] X. Liu, Y. Zhao, R. Q. Lv, and Q. Wang, "Enhancement of RI sensitivity through bending a tapered-SMF-based balloon-like interferometer," *Journal of Lightwave Technology*, 2016, 34(14): 3293–3299.

[29] S. Kiesel, K. Peters, T. Hassan, and M. Kowalsky, "Behaviour of intrinsic polymer optical fibre sensor for large-strain applications," *Measurement Science and Technology*, 2007, 18(10): 3144–3154.

[30] A. K. Sharma and B. D. Gupta, "On the performance of different bimetallic combinations in surface plasmon resonance based fiber optic sensors," *Journal of Applied Physics*, 2007, 101(9): 093111.